

# Silica–Metal Core–Shells and Metal Shells Synthesized by Porphyrin-Assisted Photocatalysis

Haorong Wang,<sup>†,‡</sup> Yujiang Song,<sup>†</sup> Zhongchun Wang,<sup>†</sup> Craig J. Medforth,<sup>§</sup> James E. Miller,<sup>†</sup> Lindsey Evans,<sup>†</sup> Peng Li,<sup>||</sup> and John A. Shelnutt<sup>\*,†,⊥</sup>

Advanced Materials Laboratory, Sandia National Laboratories, Albuquerque, New Mexico 87185, UNM/NSF Center for Micro-Engineered Materials, Department of Chemical and Nuclear Engineering, and Department of Earth and Planetary Sciences, University of New Mexico, Albuquerque, New Mexico 87131, and Department of Chemistry, University of Georgia, Athens, Georgia 30602

Received August 5, 2008. Revised Manuscript Received October 24, 2008

Uniform silica beads modified with a positively charged tin porphyrin (SnT(NMe4Py)P) adsorbed onto their surface are used as photocatalytically active templates to synthesize platinum and palladium shell and core–shell nanostructures. The cationic porphyrin SnT(NMe4Py)P serves a dual function, acting as both a photocatalyst to reduce metal ions and nucleate growth sites and as a surface modifier that promotes binding of platinum metal to the surface of the nanospheres. Hollow platinum nanoshells can then be produced by removing the silica cores using hydrofluoric acid. Magnetic silica–platinum core–shell spheres can also be prepared starting from silica spheres containing magnetite nanoparticles. The silica–porphyrin–platinum nanocomposites contain all the components necessary to produce hydrogen gas via a tin porphyrin-mediated reductive photocatalytic process using a sacrificial electron donor. However, due to instability of the SnT(NMe4Py)P, hydrogen production can only be realized when a degradation-resistant water-soluble tin porphyrin photocatalyst (SnTPPS) is added to a solution containing the nanocomposites and an electron donor.

## Introduction

Core–shell materials consisting of noble metal nanoparticle shells on submicrometer dielectric cores are an area of increasing interest because they often have properties quite distinct from homogeneous nanoparticles.<sup>1–11</sup> With their unique size-dependent optical, electronic, and catalytic properties, core–shell materials and their assemblies are promising for numerous technological applications including photonic materials,<sup>4,6,11–14</sup> surface-enhanced Raman scattering,<sup>15</sup> chemical and biological sensing,<sup>2</sup> and catalysis.<sup>16–18</sup> For example, the plasmon optical resonance spectrum of

core–shell structures can be tuned across the visible spectrum and into the infrared region by varying the ratio of the diameter of the dielectric core to the thickness of the metal overlayer.<sup>11,12</sup> Using uniform core templates such as Stöber silica spheres,<sup>19</sup> core–shell metal spheres can also be self-assembled into ordered structures to form photonic crystals.<sup>4,13,14</sup> Furthermore, removal of the dielectric cores provides a route to ordered metallic nanoshells with specific pore sizes that have uses as catalytic nanoreactors, sensors, porous electrodes, and fuel cell electrocatalysts.<sup>16</sup>

Currently, few core–shell structures made from Pt and Pd have been synthesized despite the importance of these metals in many catalytic reactions.<sup>20,21</sup> Herein, we report a new method for synthesizing uniform Pt-on-silica and Pd-on-silica core–shell structures. A uniform thin layer of Pt is obtained by using a tin porphyrin (SnT(NMe4Py)P); see

\* Corresponding author. Fax: (+1) 505-272-7077. E-mail: jasheln@unm.edu.

<sup>†</sup> Sandia National Laboratories.

<sup>‡</sup> UNM/NSF Center for Micro-Engineered Materials, University of New Mexico.

<sup>§</sup> Department of Chemical and Nuclear Engineering, University of New Mexico.

<sup>||</sup> Department of Earth and Planetary Sciences, University of New Mexico.

<sup>⊥</sup> University of Georgia.

- (1) Chen, C. W.; Chen, M. Q.; Serizawa, T.; Akashi, M. *Adv. Mater.* **1998**, *10*, 1122.
- (2) Shi, W. L.; Sahoo, Y.; Swihart, M. T.; Prasad, P. N. *Langmuir* **2005**, *21*, 1610.
- (3) Lu, L. H.; Capek, R.; Kornowski, A.; Gaponik, N.; Eychmüller, A. *Angew. Chem., Int. Ed.* **2005**, *44*, 5997.
- (4) Graf, C.; van Blaaderen, A. *Langmuir* **2002**, *18*, 524.
- (5) Pol, V. G.; Srivastava, D. N.; Palchik, O.; Palchik, V.; Slifkin, M. A.; Weiss, A. M.; Gedanken, A. *Langmuir* **2002**, *18*, 3352.
- (6) Pham, T.; Jackson, J. B.; Halas, N. J.; Lee, T. R. *Langmuir* **2002**, *18*, 4915.
- (7) Gittins, D. I.; Susha, A. S.; Schoeler, B.; Caruso, F. *Adv. Mater.* **2002**, *14*, 508.
- (8) Cassagneau, T.; Caruso, F. *Adv. Mater.* **2002**, *14*, 732.
- (9) Kobayashi, Y.; Salgueirino-Maceira, V.; Liz-Marzan, L. M. *Chem. Mater.* **2001**, *13*, 1630.
- (10) Dokoutchaev, A.; James, J. T.; Koene, S. C.; Pathak, S.; Prakash, G. K. S.; Thompson, M. E. *Chem. Mater.* **1999**, *11*, 2389.

- (11) Oldenburg, S. J.; Averitt, R. D.; Westcott, S. L.; Halas, N. J. *Chem. Phys. Lett.* **1998**, *288*, 243.
- (12) Oldenburg, S. J.; Jackson, J. B.; Westcott, S. L.; Halas, N. J. *Appl. Phys. Lett.* **1999**, *75*, 2897.
- (13) Brown, E. R.; McMahon, O. B. *Appl. Phys. Lett.* **1995**, *67*, 2138.
- (14) Wang, Y. L.; Ibsate, M.; Li, Z. Y.; Xia, Y. N. *Adv. Mater.* **2006**, *18*, 471.
- (15) Lu, L. H.; Eychmüller, A.; Kobayashi, A.; Hirano, Y.; Yoshida, K.; Kikkawa, Y.; Tawa, K.; Ozaki, Y. *Langmuir* **2006**, *22*, 2605.
- (16) Liang, H. P.; Zhang, H. M.; Hu, J. S.; Guo, Y. G.; Wan, L. J.; Bai, C. L. *Angew. Chem., Int. Ed.* **2004**, *43*, 1540.
- (17) Kim, S. W.; Kim, M.; Lee, W. Y.; Hyeon, T. *J. Am. Chem. Soc.* **2002**, *124*, 7642.
- (18) Liang, Z. J.; Susha, A.; Caruso, F. *Chem. Mater.* **2003**, *15*, 3176.
- (19) Stöber, W.; Fink, A.; Bohn, E. *J. Colloid Interface Sci.* **1968**, *26*, 62–9.
- (20) Kim, J.-H.; Chung, H.-W.; Lee, T. R. *Chem. Mater.* **2006**, *18*, 4115.
- (21) Liu, J. B.; Zhu, M. W.; Zhan, P.; Dong, H.; Dong, Y.; Qu, X. T.; Nie, Y. H.; Wang, Z. L. *Nanotechnology* **2006**, *17*, 4191.

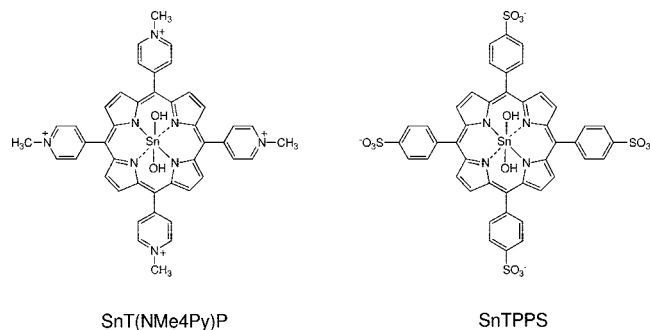


**Figure 1.** Chemical structures of the cationic water-soluble porphyrin SnT(NMe4Py)P and the anionic water-soluble porphyrin SnTPPS. Hydroxide axial ligands are shown but the ligands present in solution vary with pH.

Figure 1) adsorbed onto the silica nanospheres (and silica nanospheres containing a magnetite nanoparticle)<sup>22</sup> to photocatalytically assist the metal reduction and nucleation processes.<sup>23–26</sup> The silica cores can then be removed from the core–shell structure using hydrofluoric acid to produce uniform hollow metal spheres of desired thicknesses.

### Experimental Section

**Materials and Methods.** Reagents including tetraethoxysilane (Aldrich), SnT(NMe4Py)P (Frontier Scientific), Igepal CO-520 (Aldrich), and Ferrofluid EFH-1 (FerroTec) were used as received. Ultrapure water (Barnstead NANOpure) was used for all of the reactions. The nanostructures were characterized using TEM (200 keV JEOL 2010) and high angle annular dark field (HAADF) scanning TEM (200 keV JEOL 2010F). Samples for the electron microscopy imaging were prepared by placing drops of suspensions of the nanostructures onto standard holey carbon coated copper grids and wicking away the excess solvent with a tissue paper to remove excess solvent and dissolved salts. The surface area of the dendritic nanostructures was measured by N<sub>2</sub> adsorption experiments conducted on a Quantachrome Autosorb-6 instrument (Boynton Beach, FL). The cleaned and dried samples were degassed at 25 °C for at least 12 h at 0.01 Torr before measurement. The surface area was calculated from the Brunauer–Emmet–Teller (BET) equation using a nitrogen molecular area of 0.162 nm<sup>2</sup> and the linear region between 0.05 to 0.3 relative pressures, which gives a least-squares coefficient  $R^2 > 0.999$  for seven adsorption points.

**Preparation of SnT(NMe4Py)P-Silica Nanospheres.** Uniform-sized silica spheres were synthesized using a modification of the Stöber method.<sup>19</sup> In a typical synthesis, 2.4 mL of 30% ammonia–water was added to 40 mL of ethanol, and the solution stirred vigorously while 1.2 mL of tetraethoxysilane was added dropwise. The reaction mixture was stirred for 12 h, centrifuged at 4000 rpm, and the precipitate washed several times with water. The precipitate was then added to 40 mL of a solution of 0.3% ammonia–water and 200 μM SnT(NMe4Py)P and suspended by sonication. The suspension was left undisturbed for 10 minutes to allow complete

adsorption of the porphyrin onto the silica nanospheres, whereupon the mixture was centrifuged. The supernatant was then removed, and the precipitate mixed with 40 mL water and sonicated to produce a suspension of SnT(NMe4Py)P-modified silica nanospheres. The average diameter of the nanospheres determined from TEM images was approximately 130 nm.

Magnetic silica nanospheres consisting of a silica layer on a silica–magnetite center were synthesized in a two-step process. In the first step, silica was grown on magnetite (Fe<sub>3</sub>O<sub>4</sub>) nanoparticles approximately 5 nm in diameter using a reverse emulsion method.<sup>22</sup> In a typical procedure, mild sonication was used to dissolve 1.4 g of Igepal CO-520 in 20 mL of cyclohexane. Ferrofluid (0.02 mL) was added and the mixture sonicated for 30 min. Addition of 0.3 mL of 30% ammonia in water followed by sonication for 10 min yielded a transparent microemulsion. Tetraethoxysilane (0.16 mL) was added dropwise and the solution left undisturbed for 48 h. An aliquot of the solution (2 mL) was then mixed with 2 mL of ethanol, the magnetic silica nanoparticles were separated from solution using a magnet (similar to the procedure illustrated in Figure 6c), and the supernatant was then removed. The addition of ethanol (2 mL) followed by magnetic separation and removal of the supernatant was repeated five times. The resultant precipitate was added to 2 mL of ethanol and sonicated to produce a suspension of silica-magnetite cores with an average diameter of approximately 50 nm (determined from TEM images).

In the second step, 0.5 mL of the suspension of silica-magnetite centers in ethanol was added to 5.25 mL of ethanol and 3.45 mL of water, the mixture sonicated for 1 h, and 0.5 mL of 30% ammonia–water added. The solution was then stirred vigorously and tetraethoxysilane (0.025 mL) added four times at 12-h intervals. The reaction mixture was centrifuged for 20 min, the supernatant was removed, 0.5 mL of water and 0.1 mL of 30% ammonia–water were added, and the reaction mixture was set aside for 12 h. The solution was then centrifuged for 20 min, the supernatant was removed, and 0.1 mL of 3% ammonia–water and 0.1 mL 1 mM SnT(NMe4Py)P solution were added together with sufficient water to produce a total volume of 1 mL. After 2 h, the reaction mixture was centrifuged for 10 min and the supernatant removed. Finally, the magnetic SnT(NMe4Py)P-silica nanospheres were suspended in 0.5 mL of water by mild sonication yielding the material shown in Figure 6a.

**Titration of SnT(NMe4Py)P-Silica Nanospheres.** A solution of silica nanospheres in 0.3% ammonia–water was prepared as described previously, and 1 mL of this solution in a 2-mL vial was centrifuged at 4000 rpm. The clear supernatant was removed, and 0.1 mL of 3% ammonia–water was added, followed by the required amount of SnT(NMe4Py)P solution (1 mM) and sufficient distilled water to produce a total volume of 1 mL. The vial was sonicated for 2 min to suspend the silica nanospheres and then left undisturbed for 10 min, during which time a pink precipitate was formed. The vial was centrifuged at 4000 rpm and the supernatant analyzed using UV–visible absorption spectroscopy to determine the porphyrin concentration.

**Pt and Pd SnT(NMe4Py)P-Silica Nanospheres.** A suspension of the SnT(NMe4Py)P-silica nanospheres (0.05 mL) was added to a 4 mL glass vial containing 0.5 mL of distilled water. Aged Pt(II) solution (20 mM) (prepared by dissolving K<sub>2</sub>PtCl<sub>4</sub> in water under ambient conditions and aging at least 24 h before use, producing an equilibrium mixture of 42% Pt(H<sub>2</sub>O)<sub>2</sub>Cl<sub>2</sub>, 53% Pt(H<sub>2</sub>O)Cl<sub>3</sub><sup>-</sup>, and 5% PtCl<sub>4</sub><sup>2-</sup>)<sup>27</sup> and freshly prepared ascorbic acid solution (150 mM) were added, and the total solution volume was adjusted to 2 mL with water. The concentrations of Pt(II) in the reaction mixtures varied from 0.5 mM to 4 mM, and the concentration of ascorbic

(22) Yi, D. K.; Lee, S. S.; Papaefthymiou, G. C.; Ying, J. Y. *Chem. Mater.* **2006**, *18*, 614.

(23) Song, Y. J.; Garcia, R. M.; Dorin, R. M.; Wang, H. R.; Qiu, Y.; Shelnutt, J. A. *Angew. Chem., Int. Ed.* **2006**, *45*, 8126.

(24) Song, Y. J.; Jiang, Y. B.; Wang, H. R.; Pena, D. A.; Qiu, Y.; Miller, J. E.; Shelnutt, J. A. *Nanotechnology* **2006**, *17*, 1300.

(25) Song, Y. J.; Yang, Y.; Medforth, C. J.; Pereira, E.; Singh, A. K.; Xu, H. F.; Jiang, Y. B.; Brinker, C. J.; van Swol, F.; Shelnutt, J. A. *J. Am. Chem. Soc.* **2004**, *126*, 635.

(26) Wang, H. R.; Song, Y. J.; Medforth, C. J.; Shelnutt, J. A. *J. Am. Chem. Soc.* **2006**, *128*, 9284.

(27) Ciacchi, L. C.; Pompe, W.; Vita, A. D. *J. Am. Chem. Soc.* **2001**, *123*, 7371.

acid was 7.5 times the Pt(II) concentration. The reaction mixtures were at approximately pH 3 due to the ascorbic acid. The vial was sealed and immediately irradiated with incandescent light ( $800 \text{ nmol cm}^{-2} \text{ s}^{-1}$ ) for 30 min. The reaction solution gradually changed to a black suspension indicating that the platinum complex had been reduced.

Magnetic silica–Pt core–shell structures were synthesized by adding 0.05 mL of a suspension of the magnetic SnT(NMe4Py)P-silica nanospheres in water to 2 mL of a solution containing 1 mM Pt(II) and 7.5 mM ascorbic acid. The reaction mixture was illuminated with incandescent light ( $800 \text{ nmol cm}^{-2} \text{ s}^{-1}$ ) for 30 min. A black suspension was formed that could be separated using a magnet (see Figure 6c).

The synthesis of silica–palladium core–shell structures utilized a modified version of the reaction employed for the synthesis of the silica–platinum core–shell structures. The modifications were necessary because under the reaction conditions used for the platinization reaction the palladium salt is immediately reduced by the ascorbic acid. In the modified procedure, 0.05 mL of a suspension of the SnT(NMe4Py)P-silica nanospheres in water was added to 2 mL of a solution containing  $\text{K}_2\text{PdCl}_4$  (2 mM) and triethanolamine (TEA) (15 mM). The solution was subjected to light illumination ( $1600 \text{ nmol cm}^{-2} \text{ s}^{-1}$ ) for 1 h to photocatalytically grow Pd seed particles. During the reaction, the vial was sonicated for 10 s every 10 min to prevent precipitation of the colloid. After light illumination, 0.4 mL of a freshly prepared solution of  $\text{K}_2\text{PdCl}_4$  (10 mM) and TEA (75 mM) was added and the solution gently stirred for about 30 s. A total of 0.4 mL of ascorbic acid solution (150 mM) was then added and the suspension left undisturbed. The reaction mixture gradually changed from brown to black and a black precipitate was produced.

**Preparation of Hollow Pt Spheres.** Hollow Pt spheres were synthesized by removing the silica cores from silica nanosphere–Pt core–shell structures using hydrofluoric acid. The core–shell structures were prepared using the experimental procedure described previously with reactant concentrations of 4 mM Pt(II) and 30 mM ascorbic acid. Core–shell structures were synthesized using lower concentrations of Pt(II) produced Pt fragments rather than hollow spheres upon treatment with hydrofluoric acid.

The synthesis was carried out on a large scale to provide sufficient material for surface area characterization. In the reaction, 125 mL of a suspension of the silica–Pt core–shell structures was prepared by scaling up the procedure described previously. This mixture was then concentrated to 40, and 0.5 mL of 10% hydrofluoric acid was added. After 20 min the product was separated using a centrifuge. The product was washed 5 times with distilled water and then dried at  $60^\circ\text{C}$  for 1 h to produce the material shown in Figure 2d.

**Hydrogen Generation Experiments.** To prepare nanospheres with a low platinum loading, 2 mL of a suspension of the SnT(NMe4Py)P-silica nanospheres in water was placed in a glass reaction vial and the solution pH adjusted with 0.1 M hydrochloric acid to match the platinization reaction (pH 3). Removal of the supernatant after centrifugation then eliminated any SnT(NMe4Py)P that had dissolved at the low pH used in the platinization reaction. Next, 10 mL of water was added and the mixture sonicated, followed by the addition of 0.1 mL of  $\text{K}_2\text{PtCl}_4$  solution (20 mM) and 0.5 mL of ascorbic acid solution (150 mM). The vial was then subjected to light illumination ( $1600 \text{ mol cm}^{-2} \text{ s}^{-1}$ ) for 30 min while being gently stirred. The solution was centrifuged and the supernatant removed, with the precipitate being used in the hydrogen generation experiments. The platinum loading of the silica nanospheres is 2.4 wt % assuming that all of the Pt(II) salt is reduced and deposited on the nanospheres.

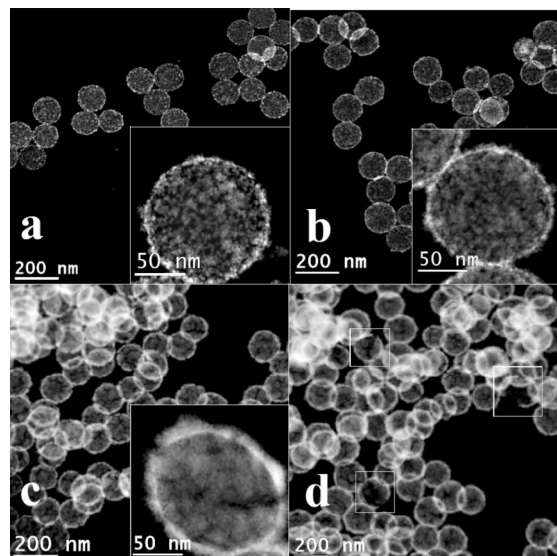


**Figure 2.** HAADF scanning TEM images of Pt grown on silica nanospheres coated with SnT(NMe4Py)P using (a) 0.5 mM, (b) 1 mM Pt, or (c) 4 mM Pt(II) complex and (d) hollow Pt shells obtained after the removal of silica from sample (c) using hydrofluoric acid. Broken shells in (d) are highlighted by the white squares.

For the hydrogen generation experiments, the silica–SnT(NMe4Py)P–Pt nanospheres were suspended in 10 mL of tin(IV) 5,10,15,20-tetrakis(4-sulfonatophenyl)porphyrin (SnTPPS) solution (40  $\mu\text{M}$ ) and placed in a 30 mL glass reaction vial. EDTA disodium salt (372 mg) was added as a sacrificial electron donor and the vial sealed and purged with argon for 20 min. The solution was then illuminated with light from an incandescent lamp ( $800 \text{ mol cm}^{-2} \text{ s}^{-1}$ ) and gently stirred. Gas samples (100  $\mu\text{L}$ ) were taken from the head space and analyzed for hydrogen using a gas chromatograph (Hewlett-Packard 5890 Series II, equipped with a packed mole SIEVE 5A column and thermal conductivity detector using argon as the carrier gas).

## Results

To generate the Pt-coated silica nanospheres, tin(IV) 5,10,15,20-tetrakis-(*N*-methyl-4-pyridyl)porphyrin(SnT(NMe4Py)P; Figure 1) is adsorbed onto the spheres and then used as a photocatalyst to assist in the growth<sup>23–26</sup> of a thin layer of Pt metal (see Figure 2). Other methods for depositing metal coatings on the surfaces of dielectric colloids include surface chemical absorption and subsequent reduction,<sup>28</sup> sonochemical deposition,<sup>5,10</sup> electroless plating deposition,<sup>9</sup> deposition of metal seed particles to facilitate metal addition,<sup>2,6</sup> and layer-by-layer self-assembly of functionalized metal nanoparticles.<sup>8,29</sup> The porphyrin-photocatalyzed deposition method has advantages such as delicate control of the amount of metal deposited to form the shell and the simplicity of the procedure.

Typically,  $\text{K}_2\text{PtCl}_4$  and ascorbic acid solutions are added to a suspension of the SnT(NMe4Py)P-treated silica nanospheres and the mixture is irradiated with visible light. Platinum metal then grows on the porphyrin-coated silica surfaces through a photocatalytic–autocatalytic process

(28) Chen, C. W.; Serizawa, T.; Akashi, M. *Chem. Mater.* **1999**, *11*, 1381.

(29) Caruso, F.; Spasova, M.; Saiguerino-Maceira, V.; Liz-Marzan, L. M. *Adv. Mater.* **2001**, *13*, 1090.

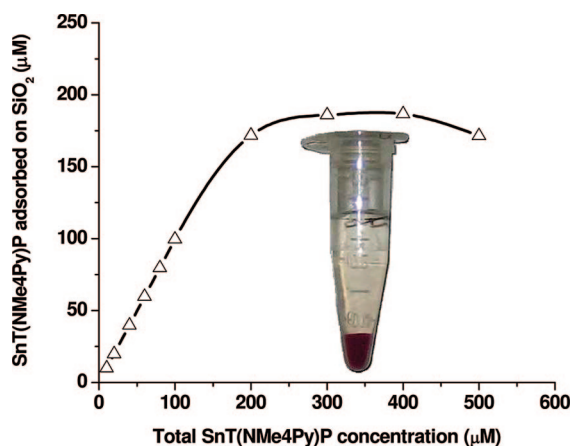


**Figure 3.** Isotherm adsorption curve for SnT(NMe4Py)P on Stöber silica spheres (8 mg/mL suspension in 0.3% ammonium hydroxide). Picture shows the pink precipitated spheres and clear supernatant.

described previously.<sup>23–26</sup> Briefly, the tin porphyrin photocatalyst molecules are excited to the triplet state and then reduced by the sacrificial electron donor to form  $\pi$ -anion radicals. These radicals then reduce the metal salt and metallize the surface of the nanospheres. The neutral porphyrins are then available to participate in additional photoreductive cycles and thus continuously deposit metal atoms to form seed nanoparticles. Once the platinum seeds reach a critical size they begin to grow autocatalytically by oxidation of ascorbic acid and reduction of Pt complex. The end result is a uniform coating of many small Pt dendrites that ultimately join to form the shell. Using different concentrations of  $K_2PtCl_4$ , the thickness of the metal shells can be varied as demonstrated by the HAADF scanning TEM images in Figure 2a–c.

Silica nanospheres prepared using the Stöber method provide a good template for adsorption of the positively charged porphyrin photocatalyst since the spheres are negatively charged<sup>30</sup> at high pH. It is probable that the SnT(NMe4Py)P forms only one or two layers on the silica nanospheres as the porphyrins are not expected to aggregate on the spheres once the negative charge on the surface has been neutralized. The adsorption of SnT(NMe4Py)P onto the silica spheres was investigated by titrating a suspension of the silica nanospheres with SnT(NMe4Py)P (Figure 3). At low porphyrin concentrations there is a loss of pink color from the solution upon the formation of a pink precipitate of porphyrin-coated silica spheres that occurs in approximately 20 min (see photograph in Figure 3). In contrast, at high porphyrin concentrations, the supernatant remains pink after the pink precipitate has formed. The saturation concentration of SnT(NMe4Py)P determined by the titration is approximately 180  $\mu$ M.

From the saturation concentration of the porphyrin and the surface area of the silica spheres we can estimate the coverage of porphyrin on the spheres. The average diameter of the silica spheres obtained from TEM images is 130 nm and the density of Stöber nanospheres is 2.0 g cm<sup>-3</sup>,<sup>31</sup> so

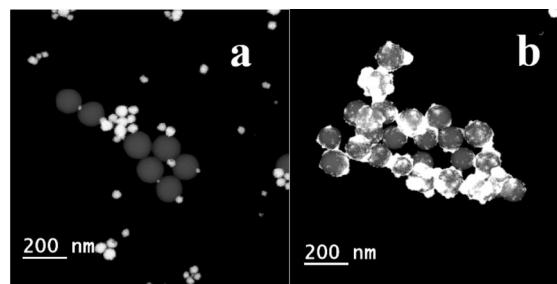


**Figure 4.** HAADF scanning TEM images of materials obtained by (a) Pt(II) reduction in a suspension of silica spheres without adsorbed SnT(NMe4Py)P and (b) Pt(II) reduction in a suspension of SnT(NMe4Py)P-modified silica spheres in the dark. The Pt(II) concentration is 1 mM in both cases and ascorbic acid is used as a sacrificial electron donor.

based on the amount of silicon precursor, the bead concentration in the titration mixture is  $\sim 3.33 \times 10^{12}$  per mL and the total bead geometrical surface area for the spheres is  $\sim 0.177$  m<sup>2</sup>. The surface area of a flat surface of a SnT(NMe4Py)P molecule is  $\sim 4$  nm<sup>2</sup> giving a surface area for the porphyrins of  $\sim 0.434$  m<sup>2</sup> at the saturation concentration of 180  $\mu$ M. The ratio of the two surface areas (a factor of 2.45) may indicate formation of more than one layer of SnT(NMe4Py)P but could also be due to other factors such as overestimation of the effective area of the porphyrin molecules (because they may stack edge-on rather than flat on the bead surface) and/or underestimation of the surface area of the spheres (due to surface roughness of the spheres). Thermogravimetric analysis of a sample of SnT(NMe4Py)P-silica nanospheres (see text and Figures S1–S3 of the Supporting Information) also yields a higher surface area ratio than that expected for an idealized monolayer of porphyrin molecules lying flat on the surface of idealized silica spheres (porphyrin surface area 0.696 m<sup>2</sup>, silica surface area 0.152 m<sup>2</sup>, ratio 4.55:1). All of these surface area ratios are consistent with no more than several layers of porphyrin on the bead surface.

Additional experiments indicate that the tin porphyrin has another role besides serving as a photocatalyst for metal reduction and seed formation. Without SnT(NMe4Py)P adsorbed on the surface of the silica spheres, ascorbic acid reduction of Pt complex produces nanoscale globular Pt dendrites of various sizes (small bright features in Figure 4a) that are typically not attached to the silica nanospheres (larger dark spheres). With porphyrin adsorbed on the silica surface but without light exposure the Pt dendrites are attached to the surfaces of the silica nanospheres (Figure 4b), but in the absence of photocatalytic seeding the dendrite size is generally larger and uncontrolled and the coverage is uneven (compare Figures 4b and 2c). These findings suggest that the tin porphyrin acts as a surface modifier to favor binding of platinum metal to the silica nanospheres. In the case of templates based on surfactant assemblies, it was initially unclear whether Pt metal prefers hydrophobic or hydrophilic regions, but subsequent studies have shown a clear preference for hydrophobic domains.<sup>23,24</sup> The results from the present studies further confirms this conclusion, as binding of SnT(NMe4Py)P to the silica nanospheres is expected to enhance the hydrophobicity of the surface of the spheres.

(30) Murai, M.; Yamada, H.; Yamanaka, J.; Onda, S.; Yonese, M.; Ito, K.; Sawada, T.; Uchida, F.; Ohki, Y. *Langmuir* **2007**, *23*, 7510.

(31) Westcott, S. L.; Oldenburg, S. J.; Lee, T. R.; Halas, N. J. *Langmuir* **1998**, *14*, 5396.

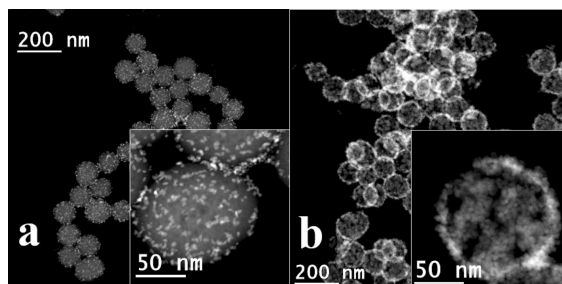


**Figure 5.** HAADF scanning TEM images of Pd-silica core-shells: (a) Pd seeded silica, (b) after shell growth.

The silica cores of the core-shell spheres shown in Figure 2a–c can be removed using hydrofluoric acid to yield the hollow Pt shells shown in the TEM image in Figure 2d. Removal of the silica was confirmed by ICP analysis of the shells that revealed only a trace amount of silica (<0.25% by weight). Brunauer–Emmett–Teller (BET) analysis of  $N_2$  absorption measurements of the Pt shells reveals a surface area of  $29 \text{ m}^2/\text{g}$ , a moderately high value for an unsupported Pt nanomaterial. These uniform shell structures may have applications as novel catalysts, especially in reactions where high mass transport is beneficial. For example, a recent report on platinum nanotubes<sup>32</sup> suggests that the hollow platinum spheres might be used in a durable unsupported oxygen reduction electrode in fuel cells. Analogous hollow Pd spheres are known to be excellent catalysts for the Suzuki reaction.<sup>17</sup>

To determine whether formation of the core-shell structures is unique to Pt, we investigated the synthesis of the analogous palladium structures. The Pd salt was found to react immediately with ascorbic acid, so a two-stage procedure was employed in which a weaker electron donor triethanolamine (TEA) was used initially to produce Pd seed particles on the silica surface by a purely photocatalytic process (Figure 5a) followed by the addition of Pd(II) complex, TEA, and ascorbic acid to further grow the seeds to form the shells (Figure 5b). The silica nanosphere–Pd core-shell structures produced using this modified procedure have less uniform coverage than the corresponding Pt systems shown in Figure 2, which is most likely due to there being a lower number of seed particles. TEA may also act as a passivating agent, especially in the second stage of the reaction since it apparently slows the reduction by ascorbic acid.

Magnetic particles can also be included inside the silica spheres to make the core-shell structures magnetic, which could be important for separation and recovery of Pt in various applications. The TEM image in Figure 6a shows silica “spheres” containing one or more 5-nm magnetite ( $\text{Fe}_3\text{O}_4$ ) nanoparticles (evident as the small dark areas near the centers of the spheres). Magnetic Pt core-shell structures (Figure 6b) were then synthesized using the same procedure described for the nonmagnetic analogs and could be readily purified by magnetic separation (Figure 6c).

Tin porphyrins are known to behave as homogeneous photocatalysts for the reduction of water.<sup>33–35</sup> In these

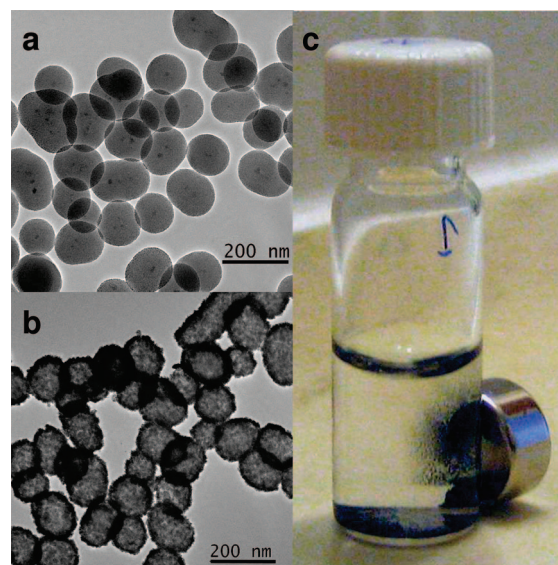


**Figure 6.** TEM images of silica beads with magnetic cores (a) and platinum shells grown on these beads (b). The photo image (c) shows the effect of a magnet on a suspension of the platinumized beads.

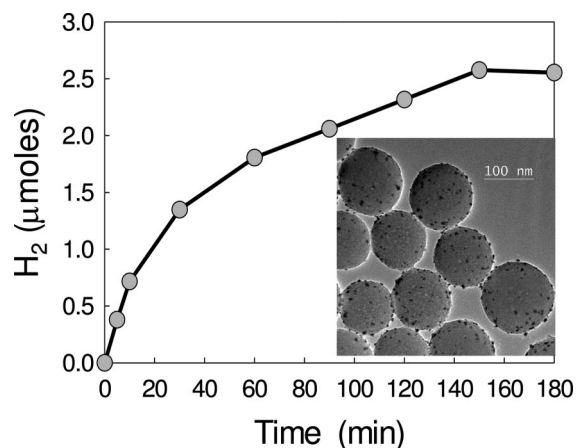


**Figure 7.** Hydrogen concentration as a function of time for silica-SnT(NMe4Py)P-Pt nanocomposites in the presence of  $40 \mu\text{M}$  SnTPPS. Inset: TEM image of silica-SnT(NMe4Py)P-Pt composites prior to use in the hydrogen generation experiments.

systems, reduction of a photoexcited tin porphyrin by a sacrificial electron donor generates a porphyrin  $\pi$ -anion radical that can donate an electron directly to colloidal platinum where protons are reduced to  $H_2$ . The photocatalytic reaction can be compared to the metal ion reduction–metal growth process previously described except that electrons from the porphyrin  $\pi$ -anion radicals ultimately reduce protons in the absence of reducible metal ions. As the silica-SnT(NMe4Py)P-Pt nanocomposites have both tin porphyrins and nanostructured platinum on their surfaces, we investigated whether they could evolve  $H_2$  in the presence of an electron donor. Using EDTA (100 mM) as the electron donor and silica spheres with a low (estimated 2.4 wt %) Pt loading (Figure 7, inset), no hydrogen was detected when the system was subjected to intense light from a tungsten lamp. Addition of more SnT(NMe4Py)P ( $40 \mu\text{M}$ ) also produced undetectable or negligible amounts of hydrogen.

(32) Chen, Z. W.; Waje, M.; Li, W. Z.; Yan, Y. S. *Angew. Chem., Int. Ed.* **2007**, *46*, 4060.

(33) Kruger, W.; Fuhrhop, J. H. *Angew. Chem., Int. Ed.* **1982**, *21*, 131.

(34) Shelnutt, J. A. *J. Am. Chem. Soc.* **1983**, *105*, 7179.

(35) Szulbinski, W.; Strojek, J. W. *Inorg. Chim. Acta* **1986**, *118*, 91.

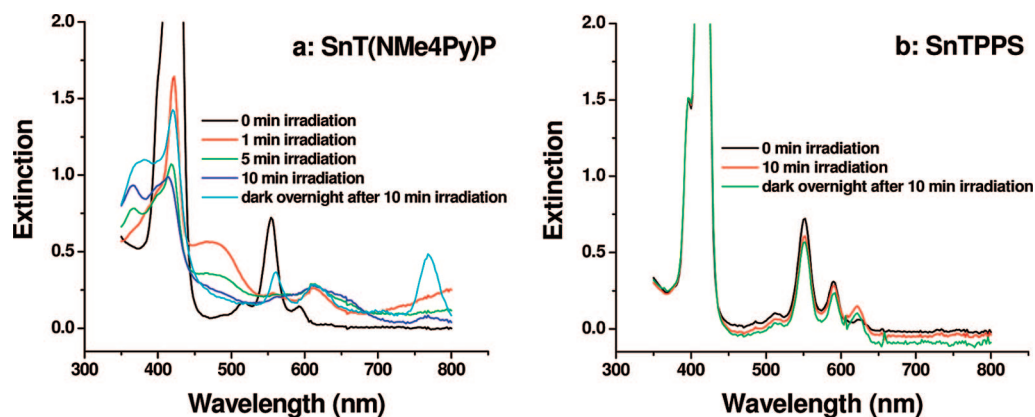


**Figure 8.** UV–visible spectra of (a) SnT(NMe4Py)P ( $40\ \mu\text{M}$  in  $10\ \text{mM}$  EDTA) and (b) SnTPPS ( $40\ \mu\text{M}$  in  $10\ \text{mM}$  EDTA) before and after irradiation with light from an incandescent lamp ( $800\ \text{mol cm}^{-2}\ \text{s}^{-1}$ ).

Control experiments in which a solution containing  $40\ \mu\text{M}$  SnT(NMe4Py)P and  $100\ \text{mM}$  EDTA as an electron donor is irradiated with white light show decomposition of the SnT(NMe4Py)P in only a few minutes (see Figure 8a). This result suggests that the nanocomposites do not generate hydrogen because the tin porphyrin complex on the spheres is decomposing in the presence of EDTA. Addition of a different water-soluble porphyrin (SnTPPS; Figure 1) that does not decompose significantly in the presence of EDTA upon irradiation for 10 min (see Figure 8b) does support the production of significant amounts of  $\text{H}_2$ ; 13 turnovers of the tin porphyrin photocatalyst are observed before hydrogen production levels off (probably due to slow decomposition of the SnTPPS, as indicated by a change in the color of the reaction mixture). Note that SnT(NMe4Py)P does not show significant decomposition (see Figure S4 of the Supporting Information) under the conditions used to produce the platinized silica–SnT(NMe4Py)P–Pt nanocomposites with ascorbic acid as the electron donor. However, ascorbic acid was not used for the hydrogen generation experiments because products of ascorbic acid oxidation may interfere with hydrogen production.

### Conclusions

In conclusion, we have synthesized silica–Pt core–shell structures using an adsorbed cationic tin porphyrin as a photocatalyst to facilitate metal growth on the surface of the silica nanospheres. When exposed to visible light in the presence of Pt complex and an electron donor, the porphyrin

photocatalytically produces Pt metal to form seed nanoparticles, which then grow autocatalytically into nanoscale Pt dendrites that join together to form a uniform thin shell. In addition to serving as a photocatalyst, the porphyrin also modifies the silica surface causing the Pt particles and dendrites to bind to the more hydrophobic porphyrin-modified surface.<sup>36</sup> The silica cores can be removed to yield hollow platinum shells. Magnetic nanoparticles can also be included in the silica cores to facilitate Pt separation and recovery. In addition, other catalytic metals (e.g., Pd) can be grown on the silica nanospheres using slightly modified versions of the method described for platinum. Facile manipulation of the structural control variables of light intensity and exposure time and metal complex concentration make this a convenient and effective method for producing sparsely metalized silica nanostructures, core–shell nanostructures, and nanoshells.

**Acknowledgment.** Sandia is multiprogram laboratory operated by Sandia Corporation, a Lockheed Martin Company, for the United States Department of Energy’s National Nuclear Security Administration, under Contract No. DEAC04-94AL85000.

**Supporting Information Available:** TG-DTA and UV–vis absorption spectra (PDF). This material is available free of charge via the Internet at <http://pubs.acs.org>.

CM802143D

(36) Garcia, R. M.; Song, Y.; Dorin, R. M.; Wang, H.; Li, P.; Qiu, Y.; van Swol, F.; Shelnutt, J. A. *Chem. Commun.* **2008**, 2535.